



OPEN ACCESS

EDITED BY

Sérgio P. Ávila,
University of the Azores, Portugal

REVIEWED BY

Francisco Jose Roig,
Universidad San Jorge, Spain
Aparna Chaudhari,
Central Institute of Fisheries Education (ICAR),
India

*CORRESPONDENCE

Tianxiang Gao
✉ gaotianxiang0611@163.com

RECEIVED 02 November 2023

ACCEPTED 22 December 2023

PUBLISHED 11 January 2024

CITATION

Zhao X, Zheng T, Song N, Qu Y and Gao T
(2024) Whole-genome survey reveals
interspecific differences in genomic
characteristics and evolution of *Pampus* fish.
Front. Mar. Sci. 10:1332250.
doi: 10.3389/fmars.2023.1332250

COPYRIGHT

© 2024 Zhao, Zheng, Song, Qu and Gao. This
is an open-access article distributed under the
terms of the [Creative Commons Attribution
License \(CC BY\)](https://creativecommons.org/licenses/by/4.0/). The use, distribution or
reproduction in other forums is permitted,
provided the original author(s) and the
copyright owner(s) are credited and that the
original publication in this journal is cited, in
accordance with accepted academic
practice. No use, distribution or reproduction
is permitted which does not comply with
these terms.

Whole-genome survey reveals interspecific differences in genomic characteristics and evolution of *Pampus* fish

Xiang Zhao¹, Tianlun Zheng², Na Song¹, Yinquan Qu³
and Tianxiang Gao^{3*}

¹The Key Laboratory of Mariculture, Ocean University of China, Ministry of Education, Qingdao, China, ²Zhejiang Fisheries Technical Extension Center, Hangzhou, Zhejiang, China, ³Fishery College, Zhejiang Ocean University, Zhoushan, Zhejiang, China

Pampus belongs to the Perciformes, Stromateoidei, and Stromateidae and are widely distributed throughout the Indian Ocean and the Western Pacific. In this study, we employed next-generation sequencing to generate comprehensive genomic data for *Pampus punctatissimus* and *Pampus echinogaster* and subsequently compared the obtained genomic information with the published data of *Pampus argenteus*. *P. echinogaster* was identified to be the largest genome size (602 Mb), heterozygosity (1.38%), and repetitive sequence ratio (33.06%), while similar genome sizes between *P. punctatissimus* (540 Mb) and *P. argenteus* (550 Mb) were observed. A total of 402,921 and 628,298 SSRs were identified for *P. punctatissimus* and *P. echinogaster*, respectively. Additionally, 1,876, 638, and 394 single-copy homologous genes were identified from *P. punctatissimus*, *P. echinogaster*, and *P. argenteus*, respectively. The KEGG enrichment results of the unique single-copy genes to the three species were significantly different in genetic information processing, protein processing, and metabolic functions. The complete mitochondrial genomes of *P. punctatissimus* and *P. echinogaster* were successfully assembled, and the resulting phylogenetic relationships align with the currently reported taxonomic status of species in the Stromateoidei. Additionally, population size analysis using PSMC revealed that *P. punctatissimus* experienced one bottleneck effect, while *P. echinogaster* underwent two bottleneck events during the Pleistocene Glacial Epoch.

KEYWORDS

Pampus, whole genome survey, single-copy genes, genomic characteristics, evolution, PSMC

1 Introduction

The *Pampus* fishes, classified under Perciformes, Stromateoidei, and Stromateidae, exhibit a wide distribution across the Indian Ocean and Western Pacific (Cui et al., 2011). All fishes of *Pampus* were economically important species and were found along the coast of China. The classification of *Pampus* fishes was further complicated due to their significant morphological similarity. Most fish taxonomists agree that *Pampus* included six species, namely, *Pampus argenteus*, *Pampus punctatissimus*, *Pampus echinogaster*, *Pampus cinereus*, *Pampus chinensis*, and *Pampus minor* (Cui et al., 2010; Karim et al., 2020). In 2013, Liu and Li (2013a) discovered a new species in the *Pampus* by comparison of morphological characteristics, named *Pampus liuorum*, and noted that this species had been previously misidentified as *P. cinereus*. Additionally, *P. argenteus* and *P. echinogaster* exhibit remarkable morphological similarities, prompting Liu and Li (2013b) to meticulously delineate the distinguishing characteristics of the former species. Recently published studies have predominantly focused on *P. argenteus*, encompassing investigations into its early developmental characteristics, biological properties, and gene functionality, among other aspects (Gao et al., 2020; Al-Abdul-Elah et al., 2021; Wang et al., 2021; Yang et al., 2021a; Yang et al., 2021b). Researchers have employed diverse molecular markers to investigate disparities among *Pampus* species. Yin et al. (2019) utilized 17,292 single-copy nuclear-encoded loci and cytochrome c oxidase subunit I (*COI*) sequences to investigate the phylogenetic relationships of *Pampus*, providing a valuable reference for *Pampus* classification. Wei et al. (2021) employed sequences of *COI* and cytochrome b (*CYTB*) to discriminate among seven *Pampus* species and authenticate their taxonomic validity. However, a single molecular marker has certain limitations in species identification (Li et al., 2013).

Recently developed rapidly high-throughput sequencing and bioinformatics analysis technology provide a practical approach to uncovering the species' whole-genome information (Chen et al., 2020; Xu et al., 2020). Whole-genome data not only enable a fundamental genomic characterization of species (Lu et al., 2016; Bi et al., 2019) but also can be used to mine mitochondrial genomes, microsatellite markers, and single-copy homologous genes (Koprek et al., 2001; Gilbert et al., 2015; Ziya Motalebipour et al., 2016; Song et al., 2018; Van Dam et al., 2021). Furthermore, the utilization of whole-genome data from a single species can also facilitate the prediction of historical population dynamics. These data provided a new perspective for resolving differences between species.

In this study, whole-genome data of *P. punctatissimus* and *P. echinogaster* were obtained by using the Illumina sequencing technique. Meanwhile, we downloaded published whole-genome data of *P. argenteus* for comparative analysis (AlMomin et al., 2016). The aims of this study were (1) to compare the whole-genome features of the three species, (2) to utilize whole-genome data for the compilation of the mitochondrial genome and analysis of phylogenetic relationships among selected species within Stromateoidei, (3) to compare the number and distribution patterns of Simple Sequence Repeats (SSRs), (4) to extract single-copy homologous genes and resolve functional differences between

species, and (5) to predict species historical dynamics. Our works uncover the differences among three *Pampus* species at the genome-wide level, which greatly enriches the genomic information of *Pampus* and provides a new case on the evolutionary biology and taxonomy.

2 Materials and methods

2.1 Ethics statement

This study does not involve the use of endangered or live animals. The *P. punctatissimus* and *P. echinogaster* samples utilized in this study were obtained from fishery production and were deceased at the time of collection. All animal experiments adhered to the guidelines and received approval from the Animal Research and Ethics Committees of the Ocean University of China.

2.2 Sample collection and genome survey sequencing

Samples of *P. punctatissimus* and *P. echinogaster* were collected in June and August 2021, respectively, in Zhoushan City, Zhejiang Province, China. The muscle tissues were preserved in 95% ethanol at -80°C , and the total genomic DNA was extracted using the standard phenol-chloroform method. The purity and concentration of DNA were detected by NanoDrop8000 microspectrophotometer and Qubit fluorometer, respectively. The high-quality DNA samples were randomly broken into fragments by Covaris ultrasonic crusher, and the whole library preparation was completed by end repair, the addition of A-tail, the addition of sequencing junction, purification, and PCR amplification. The constructed libraries were sequenced by Illumina HiSeq Nova for PE 150 (paired-end). The library construction and sequencing were performed at Wuhan Onemore-tech Co., Ltd., Wuhan, Hubei, China. The complete genomic sequencing data have been submitted to the Short Read Archive (SRA) database at the National Center for Biotechnology Information (NCBI) with accession number PRJNA853896.

2.3 Data analysis methods

In this study, raw sequencing data were processed using FASTP software to cut adaptor sequences and filter out sequences with a quality score <30 (Chen et al., 2018). After filtering out low-quality reads, we randomly selected 10,000 pairs of high-quality reads and aligned them to the NCBI nucleotide (NT) database, displaying the top 80% of identified species. All high-quality reads were utilized for K-mer analysis. K-mer calculations were performed using Jellyfish software, and K-mer frequency statistics tables were created (Marçais and Kingsford, 2011). Genome ploidy analysis was performed using Smudgeplot software (Ranallo-Benavidez et al., 2020). Genome heterozygosity and repeat ratios were calculated using GCE software (Liu et al., 2013). The estimation of genome size

was performed by analyzing the K-mer distribution curve and identifying the peaks. The case with a K-mer depth of 1 is considered an error scenario, and the obtained error rate can be utilized for genome size correction. Revised genome size can be calculated as follows: $G_{size} = N_{kmer}/C_{kmer} \times (1 - \text{Error Rate})$, where G_{size} represents the genome size, N_{kmer} denotes the total number of K-mer, and C_{kmer} signifies the peak depth.

Mitochondrial genomes were assembled from all clean sequencing reads using Mitofinder software (Allio et al., 2020) with the reference sequences downloaded from NCBI. The reference sequence accession numbers for *P. punctatissimus* and *P. echinogaster* were KF534725.1 and NC_023258.1, respectively. Assembled mitochondrial genomes were annotated using the MitoAnnotator of the Mitofish (<http://mitofish.aori.u-tokyo.ac.jp/annotation/input.html>). The mitochondrial genomes of 23 species belonging to 11 genera of Stromateoidei were retrieved from the NCBI database, encompassing a total of 13 protein-coding genes for subsequent phylogenetic analysis. Sequences were aligned using Clustal W, and a maximum likelihood tree (1,000 replicates) was constructed using MEGA X software (Kumar et al., 2018). SOAPdenovo2 software was used to assemble all clean reads into contigs and scaffolds (Luo et al., 2012). The Perl script “misa.pl” from the MISA software was utilized to identify microsatellite motifs in the *de novo* draft genome (Beier et al., 2017). The search parameters were configured to detect di-, tri-, tetra-, penta-, and hexanucleotide microsatellite motifs, requiring a minimum of 6, 5, 5, 5, and 5 repeats, respectively. Busco5 software was used to search single-copy homologous genes of *P. argenteus*, *P. punctatissimus*, and *P. echinogaster* (Simão et al., 2015). Single-copy homologous genes of each species were functionally annotated using eggNOG-Mapper based on Gene Ontology (GO) and Kyoto Encyclopedia of Genes and Genomes (KEGG) databases (Cantalapiedra et al., 2021). Subsequently, we calculated the single-copy genes specific to each species and performed KEGG enrichment analysis using the OmicShare tool (<https://www.omicshare.com/tools/>). Analysis of population size dynamics of *P. punctatissimus* and *P. echinogaster* was done using the Pairwise Sequentially Markovian Coalescent (PSMC) model, as implemented in the PSMC software (Li and Durbin, 2011). The “fq2psmcfa” and “splitfa” tools from the PSMC software were used to create the input file for the PSMC modeling. The reconstructed population history was plotted using “psmc_plot.pl” script using the substitution rate “-u 2.5e-8” and a generation time of 3 years.

3 Results

3.1 Whole-genome sequencing, k-mer analysis, and genome assembly

The indexes of the whole-genome sequencing data of the two species were shown in Table 1. The results of the NT database mapping revealed that randomly selected reads were successfully aligned with marine fish DNA, thereby demonstrating the absence of significant exogenous contamination in the data analyzed in this study (Figure 1). The 17-mer frequency distribution plot showed that *P. echinogaster* has an extremely obvious heterozygous peak (Figure 2). Both genomes of *P. punctatissimus* and *P. echinogaster* are diploid (Figure 3). The data on genome size, heterozygosity, and ratio of repetitive sequences were shown in Table 2. By comparison, *P. echinogaster* has a larger genome size, heterozygosity, and repetitive sequence ratio than the other two species, and *P. argenteus* has the lowest proportion of repetitive sequences. The measurements of total length, total number of sequences, maximum sequence length, N50 length, and N90 length for both contig and scaffold level genomes are presented in Table 3. By comparison, the total length, the total number of sequences, and the max length of sequences of *P. echinogaster* genome were larger than those of the genomes of the other two species, yet the N50 of *P. echinogaster* genome was relatively shorter than that of the other two species, especially for the length of scaffold N50.

3.2 Identification and statistics of SSR molecular markers

Based on the assembled draft genome sequences, a total of 402,921 and 628,298 SSRs were identified for *P. punctatissimus* and *P. echinogaster*, respectively. Published data showed that the 172,938 SSRs were identified in the *P. argenteus* genome (Table 4). Therefore, the frequency of SSR distribution in the genomes of *P. punctatissimus*, *P. echinogaster*, and *P. argenteus* genomes was estimated to be approximately 714.75, 956.14, and 494.03 SSRs per Mb, respectively. The SSR motif types in the genome of *P. punctatissimus* comprised 81.61% dinucleotide, 12.62% trinucleotide, 4.10% tetranucleotide, 1.48% pentanucleotide, and 0.18% hexanucleotide repeats, while their respective frequencies were 80.01%, 13.45%, 5.04%, 1.34%, and 0.16% for di-, tri-, tetra-, penta-, and hexanucleotide repeats in *P. echinogaster* genome (Figure 4).

TABLE 1 The indexes of the whole-genome sequencing data of the two species.

Species	Read number	Base count (Gb)	Q20 (%)	Q30 (%)	GC content (%)
<i>P. punctatissimus</i>	346,818,010	51.72	97.84	93.65	39.27
<i>P. echinogaster</i>	389,335,642	52.82	96.54	91.24	38.92

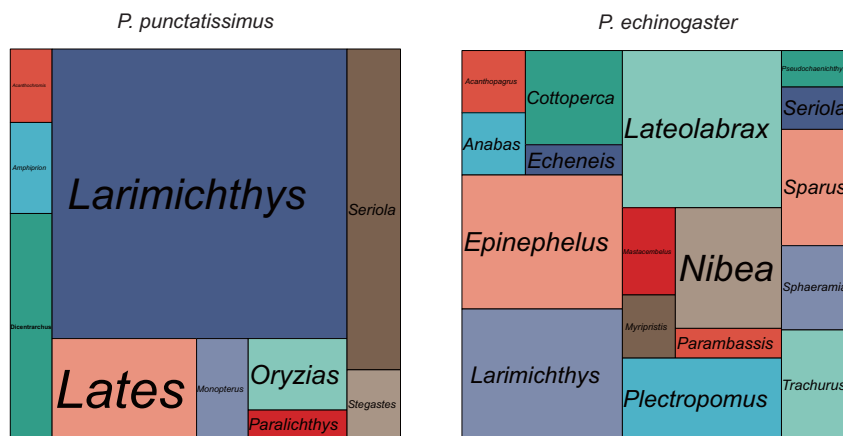


FIGURE 1 The size of each area in the mapping statistics corresponds to the number of reads that have been successfully aligned to the respective species.

3.3 Screening and functional annotation of single-copy homologous genes

Based on the draft genomes assembled in this study and published genomic data of *P. argenteus*, a total of 1,876, 638, and 394 single-copy homologous genes were identified for *P. punctatissimus*, *P. echinogaster*, and *P. argenteus*, respectively. The GO annotation results revealed that the primary terms associated with single-copy homologous genes included cellular process, single-organism process, cell, cell part, binding, and catalytic activity (Figure 5; Supplementary Table 1). KEGG annotation results indicated that single-copy homologous genes of the three species were mainly involved in the immune system, endocrine system, nervous system, glycan biosynthesis and metabolism,

translation, signal transduction, transport and catabolism, etc. (Figure 6). Interestingly, single-copy homologous genes of *P. punctatissimus* and *P. echinogaster* were also involved in environmental adaptation processes. However, very few genes in *P. argenteus* were engaged in these processes (Figure 6). A total of 1,392, 253, and 150 unique single-copy genes were screened in *P. punctatissimus*, *P. echinogaster*, and *P. argenteus*, respectively (Figure 7A). The KEGG enrichment results showed that the unique single-copy genes of *P. argenteus* did not show significant enrichment in any pathway, and the top 3 pathways containing the largest number of genes were spliceosome, protein processing in endoplasmic reticulum, and mTOR signaling pathway (Figure 7B). The unique single-copy genes of *P. punctatissimus* were significantly enriched in biosynthesis of secondary metabolites

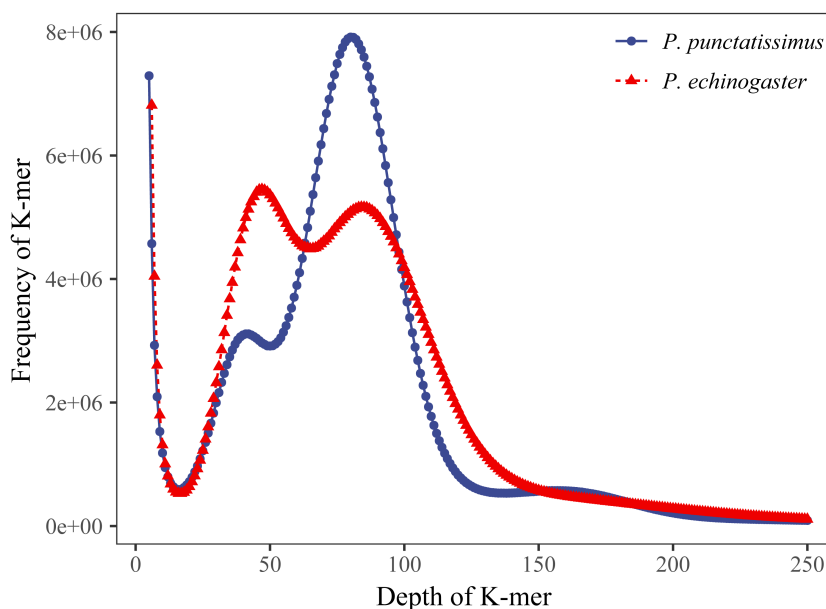


FIGURE 2 K-mer (17-mer) analysis for estimating the genome size of *P. punctatissimus* and *P. echinogaster*.

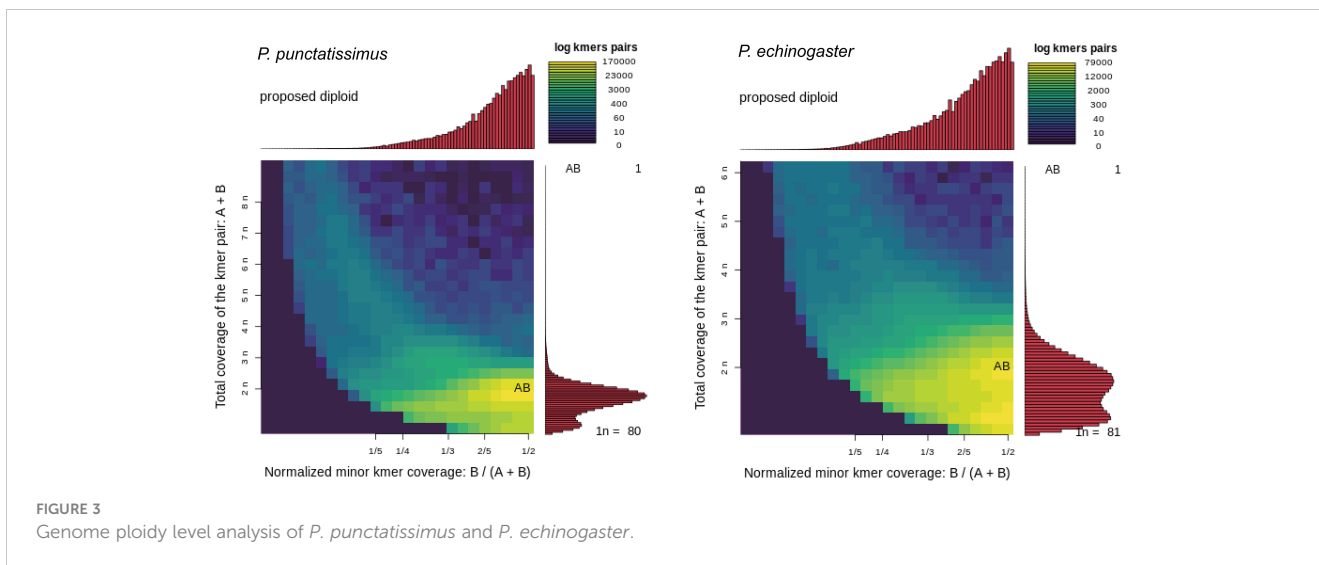


FIGURE 3 Genome ploidy level analysis of *P. punctatissimus* and *P. echinogaster*.

and purine metabolism (Figure 7C). The unique single-copy genes of *P. echinogaster* were significantly enriched in carbon metabolism (Figure 7D).

3.4 Mitochondrial genome assembly and phylogenetic analysis

The complete mitochondrial genomes of *P. punctatissimus* and *P. echinogaster* both formed closed circular molecules with lengths of 16,695 bp and 16,977 bp, respectively. The complete mitochondrial genome of both species contains 13 protein-coding genes, 22 *tRNA* genes, 2 *rRNA* genes, and 1 control region or “d-loop” (Figure 8). Except for ND6 and eight *tRNA* genes (*tRNA-Gln*, *tRNA-Ala*, *tRNA-Asn*, *tRNA-Cys*, *tRNA-Tyr*, *tRNA-Ser*, *tRNA-Glu*, *tRNA-Pro*), distributed on the light strand, the remaining mitochondrial genes were on the heavy strand. The initiation codons of *P. punctatissimus*, *P. echinogaster*, and the published *P. argenteus* mitochondrial protein-coding genes are identical. All coding genes start with ATG except for *COI*, *ND4*, and *ND6* that start with GTG. Some differences exist in the stop codons among the three species. Both *P. argenteus* and *P. echinogaster* possess eight stop codons in 13 protein-coding genes, whereas *P. punctatissimus* has only six (Figure 9). The phylogenetic tree based on 13 protein-coding genes showed that the sequences of *P. punctatissimus* and *P. echinogaster* from this study clustered with those downloaded from NCBI. The ML tree showed three major branches.

As expected, all Stomateidae fishes clustered into one group, and *Pampus* and *Peprilus* fishes were the most closely related. Tetragonuridae, Amarsipidae, Ariommatidae, and Nomeidae fishes clustered into one group, and all Centrolophidae clustered into another group (Figure 10). The phylogenetic relationships were consistent with the currently reported taxonomic status of the Stomateoidei.

3.5 Population size dynamics of *P. punctatissimus* and *P. echinogaster*

The PSMC model was employed to infer the historical fluctuations in the effective population size (*N_e*) of *P. punctatissimus* and *P. echinogaster* (Figure 11). The PSMC results showed that *P. punctatissimus* and *P. echinogaster* experienced multiple bottleneck effects over the past million years, with their effective population size fluctuating periodically. The effective population size of *P. punctatissimus* peaked approximately 4×10^4 years ago and subsequently started to decline. The decline accelerated after the last glacial maximum (2.1×10^4 years ago), an extremely cold geological period. Interestingly, two peaks in the effective population size of *P. echinogaster* occurred over the past million years. The effective population size of *P. echinogaster* peaked during the last interglacial period ($1.1\text{--}1.3 \times 10^5$ years ago), a relatively warm geological period, and then started to decline. When the last glacial period started (7×10^4 years ago), the effective

TABLE 2 The genome size, heterozygosity, and ratio of repetitive sequences of the three species.

Species	Kmer depth	Revised genome size (Mb)	Heterozygous ratio (%)	Repeat sequences ratio (%)	
<i>P. punctatissimus</i>	65	540	0.71	30.22	This study
<i>P. echinogaster</i>	77	602	1.38	33.07	
<i>P. argenteus</i>	67	550	\	11.06	AlMomin et al., 2016

“\” means these data are not shown in the reference.

TABLE 3 The genome result of assembly in *P. punctatissimus*, *P. echinogaster*, and *P. argenteus*.

Species		Total length (bp)	Total number	Max length (bp)	N50 length (bp)	N90 length (bp)	
<i>P. punctatissimus</i>	Contig	570,410,222	1,410,074	36,701	812	136	This study
	Scaffold	557,429,401	638,767	71,913	6088	201	
<i>P. echinogaster</i>	Contig	667,683,538	3,147,714	15,384	220	117	
	Scaffold	645,487,227	2,067,357	38,508	528	124	
<i>P. argenteus</i>	Contig	694,937,334	2,097,109	18,596	499	146	AlMomin et al., 2016
	Scaffold	350,058,665	298,141	33,073	1584	549	

population size of *P. echinogaster* began to rise, reaching the second peak approximately 4×10^4 years ago. Close to the last glacial maximum, there was a significant decrease in the effective population size of *P. echinogaster*.

4 Discussion

The genomic resources of *Pampus* fishes are extremely scarce, and only the *P. argenteus* genome has been published. Whole-genome survey sequencing has emerged as a rapid and cost-effective technology for acquiring complete genomes of various species (Jo et al., 2021; Zhao et al., 2022). The whole-genome data of *P.*

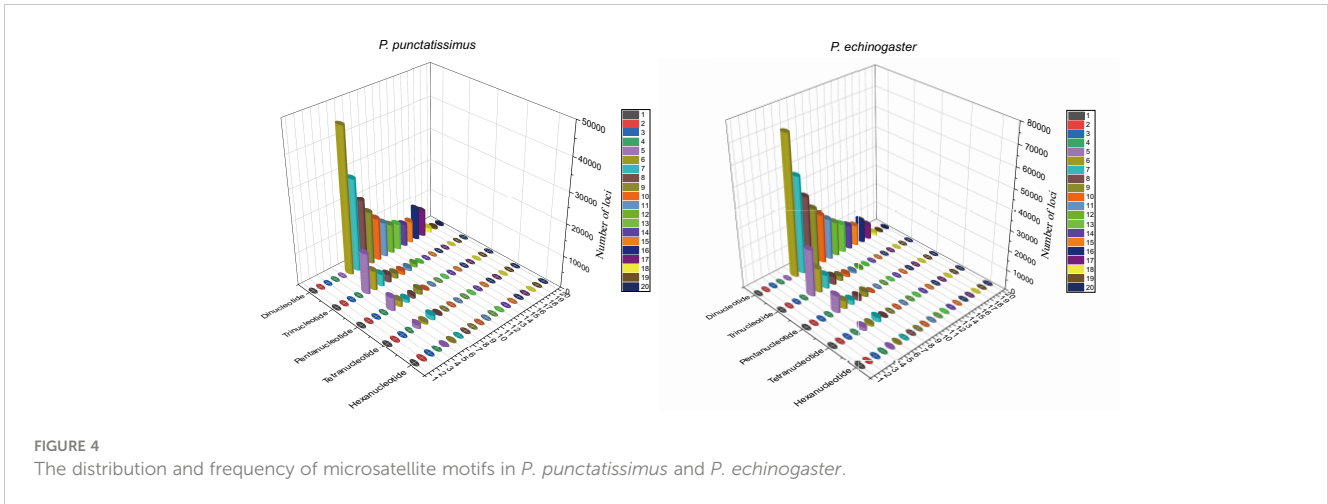
punctatissimus and *P. echinogaster* were obtained using whole-genome survey sequencing technology in this study. The raw data exhibited high quality, with an effective rate, Q20, and Q30 all exceeding 90%, indicating their suitability for subsequent analysis. The randomly selected sequencing reads were all mapped to sequences of closely related species, indicating that there is no exogenous contamination of sequencing data. The heterozygosity ratio and repeat sequences ratio in the *P. punctatissimus* genome were 0.71% (between 0.5% and 0.8%) and 30.22% (<50%), respectively. Therefore, the *P. punctatissimus* genome belongs to the micro heterozygous genome (Simpson, 2014). However, the heterozygosity of the *P. echinogaster* genome was 1.38% (>0.8%), and we considered it to be a highly heterozygous genome. The three *Pampus* species differ in genome size, and the observed discrepancy may be attributed to variations in the composition of repetitive sequences and occurrences of transposon insertions (Shao et al., 2019). Repeated sequences and high heterozygous regions can affect genome integrity during assembly (Jia et al., 2021). Therefore, the sequencing depth should be increased in the future assembly of the *P. echinogaster* and *P. punctatissimus* genomes.

This study was the first to assemble the draft genomes of *P. punctatissimus* and *P. echinogaster*. Due to the limitations of using only Illumina sequencing data, the draft scaffold genomes of the three *Pampus* species had lower N50 and N90 lengths compared to other published complete fish genomes (Fan et al., 2018; Bian et al., 2020; Prost et al., 2020). *P. echinogaster* genome has the lowest N50 and N90 indices possibly due to its higher heterozygosity and repeat sequence ratio. The scaffold draft genomes were used to identify SSRs. The large difference in SSR distribution frequencies between *P. punctatissimus* and *P. echinogaster* may be one of the potential reasons for the difference in genome size between the two species. The scaffold assembly data for the published *P. argenteus* genome were poor, with only 63.7% of the complete genome in sequence length, and therefore has the lowest number of SSRs. Similar to other studies, the motif types of SSRs in *P. punctatissimus*, *P. echinogaster*, and published *P. argenteus* genomes were dinucleotide (Choi et al., 2021; Huang et al., 2022). These SSR data will be crucial for developing molecular markers in *Pampus* fishes, but further validation studies with diverse populations are necessary.

Single-copy genes refer to genes that have a small number of copies in the genome, one or a few, and most are housekeeping genes belonging to the organism (Huang et al., 2019). The

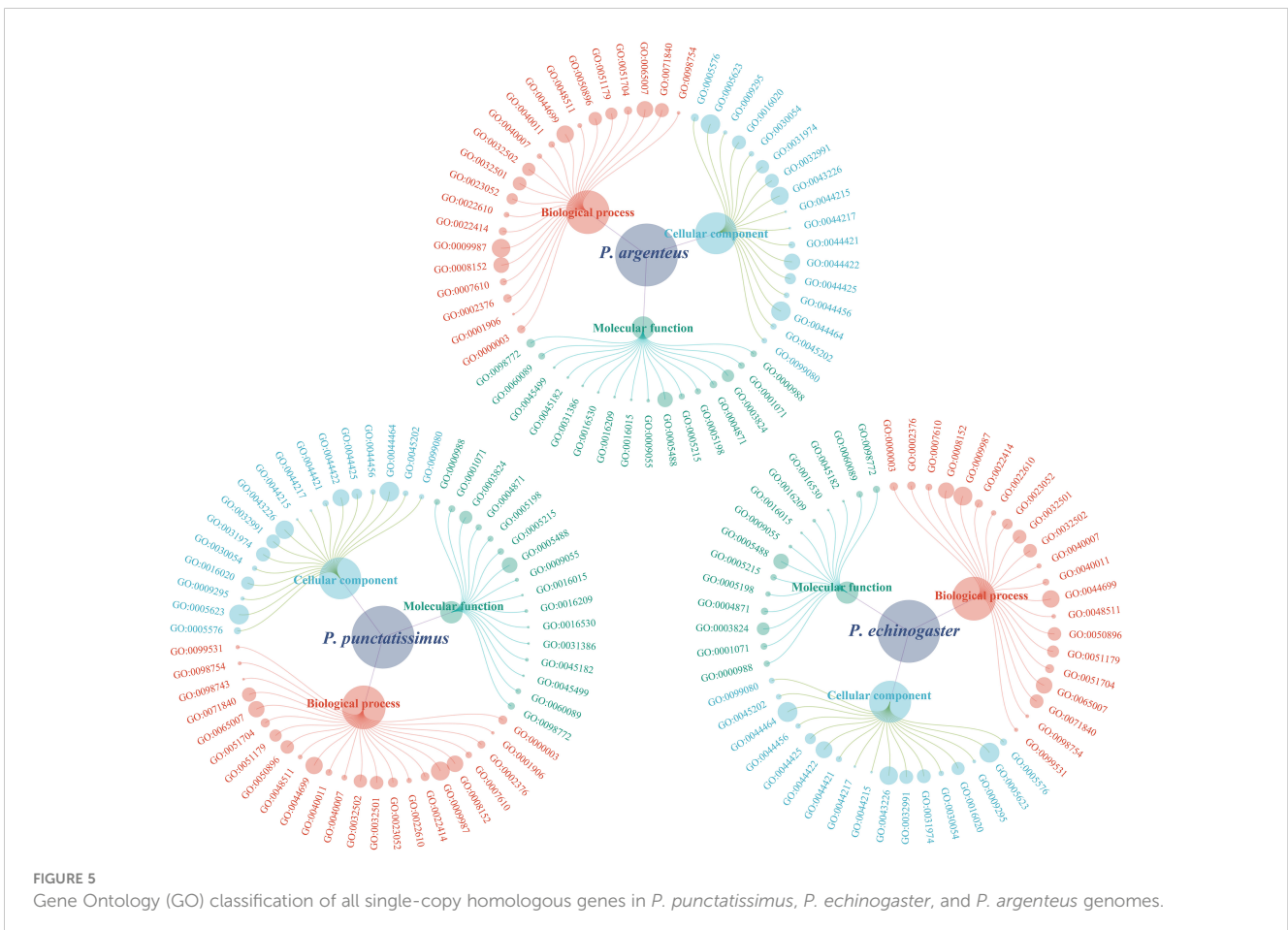
TABLE 4 Statistics of microsatellite recognition results.

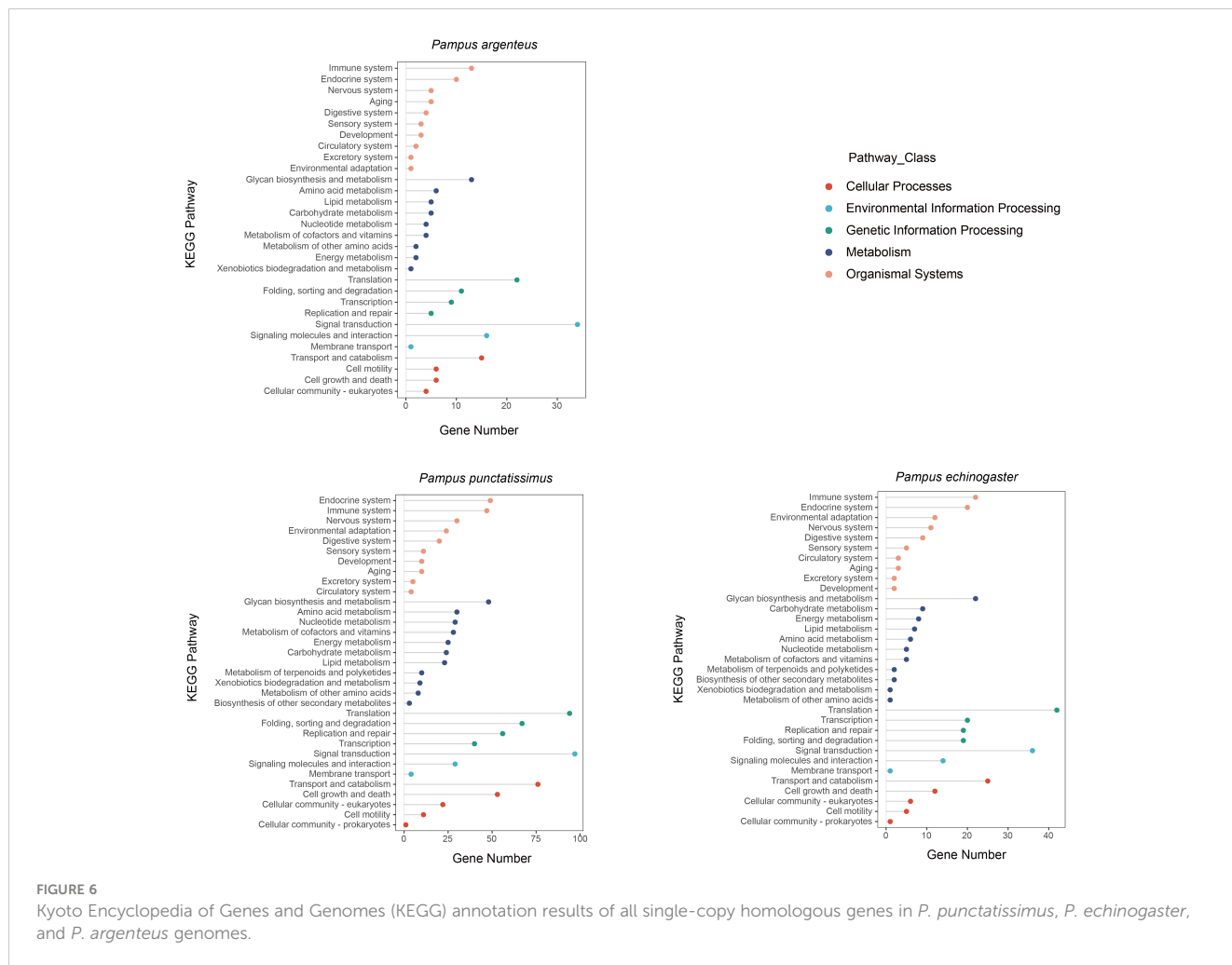
	This study		AlMomin et al., 2016
	<i>P. punctatissimus</i>	<i>P. echinogaster</i>	<i>P. argenteus</i>
Total number of sequences examined	638,767	2,067,357	298,141
Total size of examined sequences (bp)	563,723,050	657,780,705	350,058,665
Total number of identified SSRs	402,921	628,298	172,938
Number of SSR containing sequences	155,421	433,621	107,087
Number of sequences containing more than 1 SSR	66,039	102,919	38,890
Number of SSRs present in compound formation	46,375	73,417	14,743



regulation of normal life activities in organisms relies on these essential genes. Single-copy homologous genes are highly conserved during speciation, and their divergence directly leads to the formation of new species (Fitch, 1970). Dissecting the functions of single-copy homologous genes helps us to understand the differences between species. In this study, single-copy homologous gene datasets of *P. punctatissimus*, *P. echinogaster*, and *P. argenteus* were generated based on whole-genome data, and functional

annotation and enrichment analysis were performed. The number of single-copy homologous genes varied greatly among the three species, with the largest number of single-copy genes in *P. punctatissimus* and the smallest number in *P. argenteus*. However, the GO terms and KEGG pathways annotated to single-copy genes of the three species were similar and involved various aspects of life activities. Interestingly, the number of single-copy genes involved in environmental adaptation processes in *P. argenteus* was very low.





Several studies have identified several functional genes of *P. argenteus* that adapt to changes in seawater temperature and salinity (Li et al., 2020; Zhang et al., 2022). Most of these genes are not in our single-copy gene dataset. Therefore, we hypothesized that *P. argenteus* may have different regulatory mechanisms for environmental adaptation from other *Pampus* fishes. We look forward to future studies on environmental adaptations in *Pampus* fishes to verify our speculations. In addition, this study constructed single-copy homologous gene datasets unique to the three species. The unique single-copy genes of *P. argenteus* were not significantly enriched in any pathway, but the top 3 pathways containing the largest number of genes were spliceosome, protein processing in endoplasmic reticulum, and mTOR signaling pathway. Both spliceosome and protein processing in endoplasmic reticulum were associated with gene expression processes (Will and Lührmann, 2011; Braakman and Hebert, 2013). The mTOR signaling pathway serves as a master regulator of cell metabolism, growth, proliferation, and survival, and the mTOR complex 1 (*mTORC1*) plays a key role in protein synthesis (Chaturantabut et al., 2019). We proposed the conjecture that the gene expression process may differ between *P. argenteus* and other *Pampus* fishes. The unique single-copy genes of *P. punctatissimus* and *P. echinogaster* were enriched in different metabolic pathways,

suggesting that there may be some differences in the processes of substance metabolism between the two species. Dissecting the functions of single-copy homologous genes helps us to understand the differences between species.

The abundance of mitochondria in animal cells results in a higher sequencing depth for mitochondrial genomes compared to nuclear genes, enabling us to assemble a complete mitochondrial genome with ample data. Currently, the whole mitochondrial genomes of *P. punctatissimus* and *P. echinogaster* assembled based on the primer-walking method have been published (Liu et al., 2015; Li et al., 2016). The mitochondrial genomes of *P. punctatissimus* and *P. echinogaster* were assembled for the first time in this study using whole-genome sequencing data, which is consistent with the structure of previously published mitochondrial genomes. However, we found that the sequence of the mitochondrial D-loop region assembled in this study was longer and less accurate than the published sequences by sequence comparison. This may be due to the large individual variation in the D-loop region and the shorter fragment of the Illumina sequencing data. Although the method of assembling mitochondrial genome based on Illumina sequencing data has some limitations, it is more efficient and less costly than traditional methods. The phylogenetic tree based on 13 protein-

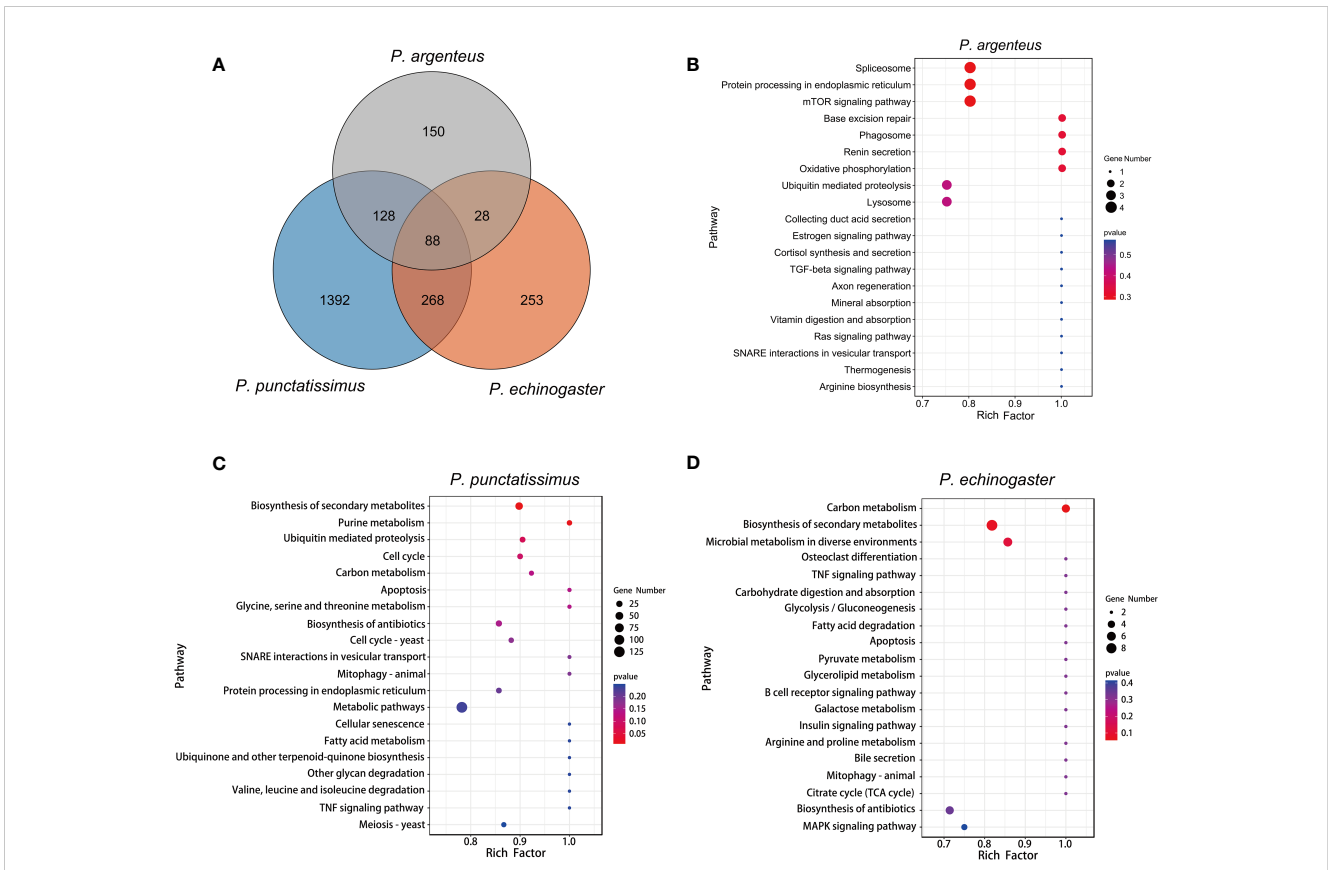


FIGURE 7 (A) represents an overview of single-copy genes in three *Pampus* species based on Venn diagrams. (B-D) represent the Kyoto Encyclopedia of Genes and Genomes (KEGG) enrichment results of the unique single-copy genes of the *P. argenteus*, *P. punctatissimus*, and *P. echinogaster* genomes, respectively.

coding genes indicated that the assembly of protein-coding genes of *P. punctatissimus* and *P. echinogaster* in this study was accurate. The phylogenetic relationships were consistent with the currently reported taxonomic status of species in the Stromateoidei (Cui et al., 2011).

Population dynamics in the genetic and evolutionary biology have long been a prominent area of research. We employed the PSMC model to infer historical fluctuations in the effective population size of *P. punctatissimus* and *P. echinogaster*. Our results suggested that *P. punctatissimus* and *P. echinogaster* experienced one and two bottleneck

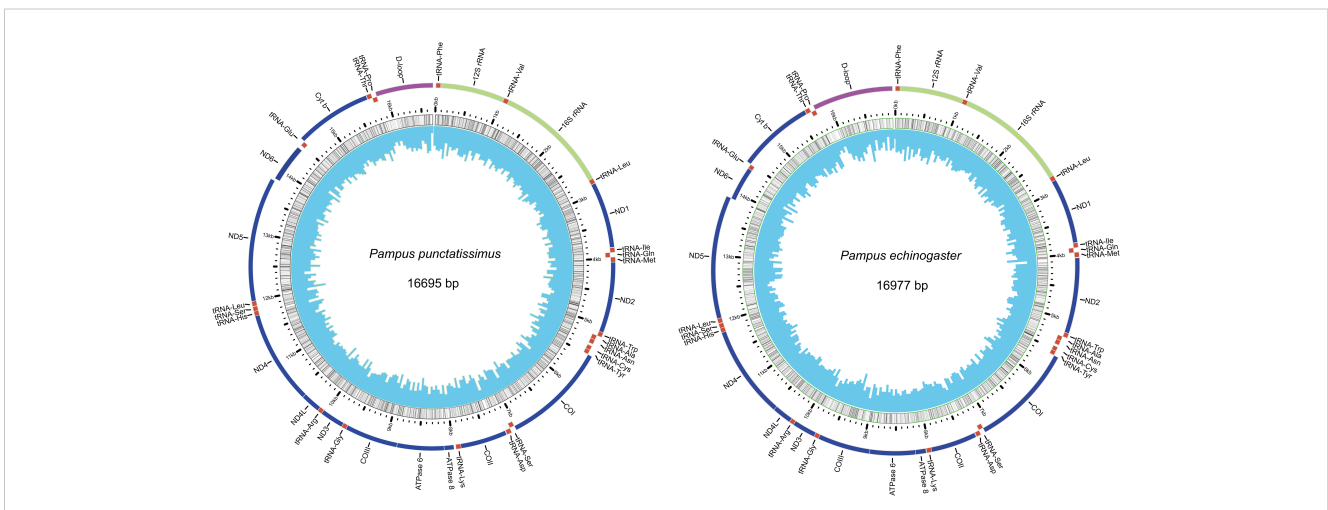


FIGURE 8 Mitochondrial genome organization of *P. punctatissimus* and *P. echinogaster*.

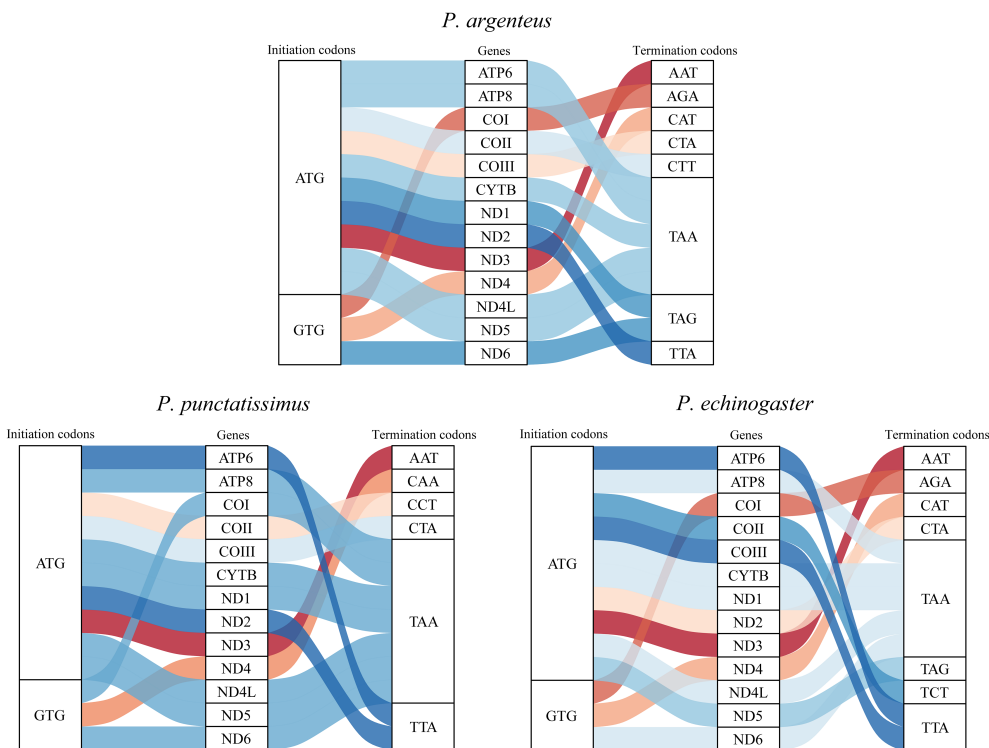


FIGURE 9 The initiation and termination codons of 13 protein-coding genes of *P. argenteus*, *P. punctatissimus*, and *P. echinogaster*.

effects during the Pleistocene Glacial Epoch, respectively. We hypothesized that the habitats of *P. punctatissimus* and *P. echinogaster* differed significantly during the Pleistocene Glacial Epoch. The unstable climate of the last interglacial period had a large impact on *P. echinogaster*, resulting in a small decline in its population size. *P. echinogaster* may be forced to migrate to more suitable sea areas, and subsequently, population size increases again. The accumulation of new mutations, however, occurs at a remarkably slow pace within a species (Latta et al., 2010). Therefore, we hypothesized that the loss of genetic diversity due to the bottleneck effect may not recover rapidly

with increasing population size. A study suggests that lower genetic diversity may lead to a reduced ability of species to adapt to climate change (Foo and Byrne, 2016). So, the population size of *P. echinogaster* declined sharply during the Last Glacial Maximum due to dramatic climate change. Unlike *P. echinogaster*, climate change during the Last Interglacial did not have a large impact on *P. punctatissimus*, and its population size continued to increase. Until the Last Glacial Maximum, sea level dropped nearly approximately 100 meters and offshore fish habitat was lost extensively, the population size of *P. punctatissimus* decreased dramatically (Hoareau et al., 2012). There was still no trend

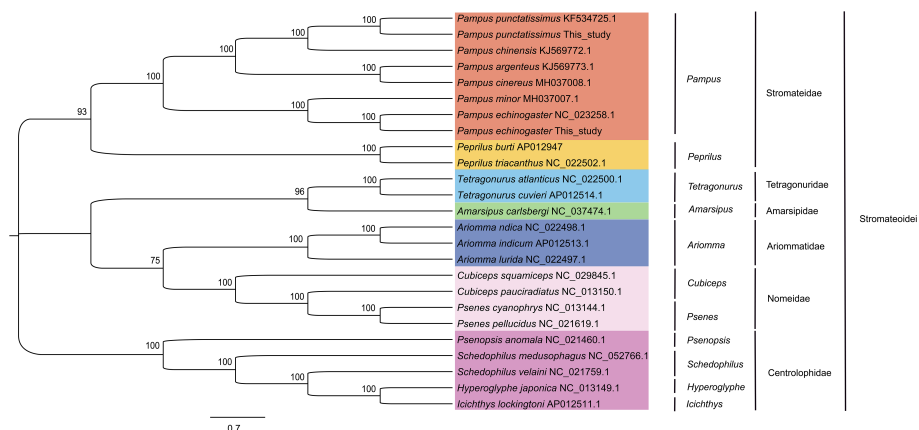


FIGURE 10 Phylogenetic trees based on 13 protein-coding genes from mitochondrial genomes of Stromateoidei species were inferred using the maximum likelihood method.

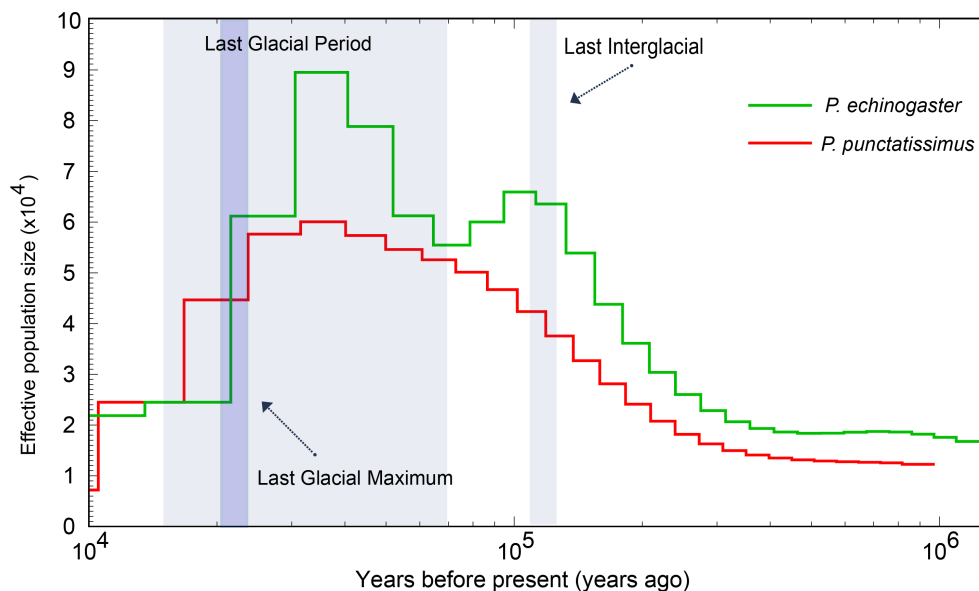


FIGURE 11
Demographic history of *P. punctatissimus* and *P. echinogaster* in this study.

of recovery in the population size of both *P. punctatissimus* and *P. echinogaster* by 10,000 years ago.

5 Conclusions

In this study, genomic survey analysis of *P. punctatissimus* and *P. echinogaster* were performed by high-throughput sequencing. Published *P. argenteus* genomic data were also used for comparative analysis. The *P. punctatissimus* genome belongs to the micro heterozygous genome, and the *P. echinogaster* genome was highly heterozygous. Genomic characteristics, SSR types and numbers, single-copy gene numbers, and functions of the three *Pampus* fishes were significantly different. The inclusion of the assembled mitochondrial genome not only enhances the genetic resources available for *Pampus* fishes but also provides further evidence supporting their taxonomic classification. A large number of SSR loci, shared single-copy homologous genes, and 13 mitochondrial protein-coding genes can be used as potential markers to differentiate the three *Pampus* fish species. The PSMC analysis revealed that *P. punctatissimus* and *P. echinogaster* underwent one and two bottleneck events, respectively, during the Pleistocene Glacial Epoch. This study provides a valuable data reference for the complete genome assembly of *P. punctatissimus* and *P. echinogaster*, offering novel insights to resolve interspecific differences among *Pampus* fishes.

Data availability statement

The original contributions presented in the study are publicly available. This data can be found here: <https://www.ncbi.nlm.nih.gov/genbank/>, PRJNA853896.

Ethics statement

The animal studies were approved by Guidelines for Experimental Animals of the Ministry of Science and Technology. The studies were conducted in accordance with the local legislation and institutional requirements. Written informed consent was obtained from the owners for the participation of their animals in this study.

Author contributions

XZ: Data curation, Formal analysis, Methodology, Visualization, Writing – original draft, Writing – review & editing. TZ: Conceptualization, Formal analysis, Investigation, Writing – review & editing. NS: Conceptualization, Methodology, Writing – review & editing, Formal analysis. YQ: Data curation, Formal analysis, Methodology, Writing – review & editing. TG: Conceptualization, Data curation, Funding acquisition, Methodology, Project administration, Writing – review & editing.

Funding

The author(s) declare financial support was received for the research, authorship, and/or publication of this article. This work was supported by the National Key Research and Development Program of China (2023YFD2401900).

Conflict of interest

The authors declare that the research was conducted in the absence of any commercial or financial relationships that could be construed as a potential conflict of interest.

Publisher's note

All claims expressed in this article are solely those of the authors and do not necessarily represent those of their affiliated

organizations, or those of the publisher, the editors and the reviewers. Any product that may be evaluated in this article, or claim that may be made by its manufacturer, is not guaranteed or endorsed by the publisher.

Supplementary material

The Supplementary Material for this article can be found online at: <https://www.frontiersin.org/articles/10.3389/fmars.2023.1332250/full#supplementary-material>

References

- Al-Abdul-Elah, K., Hossain, M. A., and Akatsu, S. (2021). Recent advances in artificial breeding and larval rearing of silver pomfret *Pampus argenteus* (Euphrasen 1788) in Kuwait. *J. Biol. Sci.* 28 (10), 5808–5815. doi: 10.1016/j.sjbs.2021.06.026
- Allio, R., Schomaker-Bastos, A., Romiguier, J., Prosdocimi, F., Nabholz, B., and Delsuc, F. (2020). MitoFinder: Efficient automated large-scale extraction of mitogenomic data in target enrichment phylogenomics. *Mol. Ecol. Res.* 20 (4), 892–905. doi: 10.1111/1755-0998.13160
- AlMomin, S., Kumar, V., Al-Amad, S., Al-Hussaini, M., Dashti, T., Al-Enezi, K., et al. (2016). Draft genome sequence of the silver pomfret fish, *Pampus argenteus*. *Genome* 59 (1), 51–58. doi: 10.1139/gen-2015-0056
- Beier, S., Thiel, T., Münch, T., Scholz, U., and Mascher, M. (2017). MISA-web: a web server for microsatellite prediction. *Bioinformatics* 33, 2583–2585. doi: 10.1093/bioinformatics/btx198
- Bi, Q., Zhao, Y., Cui, Y., and Wang, L. (2019). Genome survey sequencing and genetic background characterization of yellow horn based on next-generation sequencing. *Mol. Biol. Rep.* 46 (4), 4303–4312. doi: 10.1007/s11033-019-04884-7
- Bian, L., Li, F., Ge, J., Wang, P., Chang, Q., Zhang, S., et al. (2020). Chromosome-level genome assembly of the greenfin horse-faced filefish (*Thamnaconus septentrionalis*) using Oxford Nanopore PromethION sequencing and Hi-C technology. *Mol. Ecol. Resour.* 20 (4), 1069–1079. doi: 10.1111/1755-0998.13183
- Braakman, I., and Hebert, D. N. (2013). Protein folding in the endoplasmic reticulum. *CSH. Perspect. Biol.* 5 (5), a013201. doi: 10.1101/cshperspect.a013201
- Cantalapiedra, C. P., Hernández-Plaza, A., Letunic, I., Bork, P., and Huerta-Cepas, J. (2021). eggNOG-mapper v2: functional annotation orthology assignments and domain prediction at the metagenomic scale. *Mol. Biol. Evol.* 38 (12), 5825–5829. doi: 10.1093/molbev/msab293
- Chaturantabut, S., Shwartz, A., Evason, K. J., Cox, A. G., Labella, K., Schepers, A. G., et al. (2019). Estrogen activation of G-protein-coupled estrogen receptor 1 regulates phosphoinositide 3-kinase and mTOR signaling to promote liver growth in zebrafish and proliferation of human hepatocytes. *Gastroenterology* 156 (6), 1788–1804e13. doi: 10.1053/j.gastro.2019.01.010
- Chen, B., Sun, Z., Lou, F., Gao, T., and Song, N. (2020). Genomic characteristics and profile of microsatellite primers for *Acanthogobius ommaturus* by genome survey sequencing. *Biosci. Rep.* 40 (11), BSR20201295. doi: 10.1042/BSR20201295
- Chen, S., Zhou, Y., Chen, Y., and Gu, J. (2018). fastp: an ultra-fast all-in-one FASTQ preprocessor. *Bioinformatics* 34 (17), i884–i890. doi: 10.1093/bioinformatics/bty560
- Choi, E., Kim, S. H., Lee, S. J., Jo, E., Kim, J., Kim, J. H., et al. (2021). A first genome survey and genomic SSR marker analysis of *Trematopus loennbergii* Regan 1913. *Anim. (Basel)* 11 (11), 3186. doi: 10.3390/ani11113186
- Cui, Z., Liu, Y., Li, C. P., and Chu, K. H. (2011). Species delineation in *Pampus* (Perciformes) and the phylogenetic status of the stromateoidei based on mitogenomics. *Mol. Biol. Rep.* 38 (2), 1103–1114. doi: 10.1007/s11033-010-0207-y
- Cui, Z., Yuan, L., Jing, L., and Luan, W. (2010). Molecular identification of *Pampus* fishes (Perciformes Stromateidae). *Ichthyol. Res.* 57 (1), 32–39. doi: 10.1007/s10228-009-0119-9
- Fan, G., Chan, J., Ma, K., Yang, B., Zhang, H., Yang, X., et al. (2018). Chromosome-level reference genome of the Siamese fighting fish *Betta splendens* a model species for the study of aggression. *GigaScience* 7 (11), giy087. doi: 10.1093/gigascience/giy087
- Fitch, W. M. (1970). Distinguishing homologous from analogous proteins. *Syst. Zool.* 19, 99–113. doi: 10.2307/2412448
- Foo, S. A., and Byrne, M. (2016). Acclimatization and adaptive capacity of marine species in a changing ocean. *Adv. Mar. Biol.* 74, 69–116. doi: 10.1016/bs.amb.2016.06.001
- Gao, Q., Tang, Q., Zhao, M., Min, M., Wang, Q., Peng, S., et al. (2020). Molecular characterization of TLR3 and TRIL in silvery pomfret (*Pampus argenteus*) and their expression profiles in response to bacterial components. *Int. J. Biol. Macromol.* 155, 805–813. doi: 10.1016/j.ijbiomac.2020.03.246
- Gilbert, P. S., Chang, J., Pan, C., Sobel, E. M., Sinsheimer, J. S., Faircloth, B. C., et al. (2015). Genome-wide ultraconserved elements exhibit higher phylogenetic informativeness than traditional gene markers in percomorph fishes. *Mol. Phylogenet. Evol.* 92, 140–146. doi: 10.1016/j.ympev.2015.05.027
- Hoareau, T. B., Boissin, E., and Berrebi, P. (2012). Evolutionary history of a widespread Indo-Pacific goby: the role of Pleistocene sea-level changes on demographic contraction/expansion dynamics. *Mol. Phylogenet. Evol.* 62 (1), 566–572. doi: 10.1016/j.ympev.2011.10.004
- Huang, G., Cao, J., Chen, C., Wang, M., Liu, Z., Gao, F., et al. (2022). Genome survey of *Misgurnus anguillicaudatus* to identify genomic information simple sequence repeat (SSR) markers and mitochondrial genome. *Mol. Biol. Rep.* 49 (3), 2185–2196. doi: 10.1007/s11033-021-07037-x
- Huang, Y., Feulner, P., Eizaguirre, C., Lenz, T. L., Bornberg-Bauer, E., Milinski, M., et al. (2019). Genome-wide genotype-expression relationships reveal both copy number and single nucleotide differentiation contribute to differential gene expression between stickleback ecotypes. *Genome. Biol. Evol.* 11 (8), 2344–2359. doi: 10.1093/gbe/evz148
- Jia, C., Yang, T., Yanagimoto, T., and Gao, T. (2021). Comprehensive draft genome analyses of three rockfishes (Scorpaeniformes *Sebastes*) via genome survey sequencing. *Curr. Issues. Mol. Biol.* 43 (3), 2048–2058. doi: 10.3390/cimb43030141
- Jo, E., Lee, S. J., Choi, E., Kim, J., Lee, S. G., Lee, J. H., et al. (2021). Whole genome survey and microsatellite motif identification of *Artemia franciscana*. *Biosci. Rep.* 41 (3), BSR20203868. doi: 10.1042/BSR20203868
- Karim, E., Liu, Q., Mahmud, Y., Shamsuzzaman, M. M., and Khatun, M. H. (2020). Comparative assessment of population biology of three popular pomfrets species *Pampus argenteus* *Pampus chinensis* and *parastromateus* *Niger* of the bay of Bengal Bangladesh. *Iran. J. Fish. Sci.* 19 (2), 793–813. doi: 10.22092/ijfs.2018.119873
- Koprek, T., Rangel, S., McElroy, D., Louwse, J. D., Williams-Carrier, R. E., and Lemaux, P. G. (2001). Transposon-mediated single-copy gene delivery leads to increased transgene expression stability in barley. *Plant Physiol.* 125 (3), 1354–1362. doi: 10.1104/pp.125.3.1354
- Kumar, S., Stecher, G., Li, M., Knyaz, C., and Tamura, K. (2018). MEGA X: Molecular evolutionary genetics analysis across computing platforms. *Mol. Biol. Evol.* 35 (6), 1547–1549. doi: 10.1093/molbev/msy096
- Latta, L. C., Fisk, D. L., Knapp, R. A., and Pfrender, M. E. (2010). Genetic resilience of daphnia populations following experimental removal of introduced fish. *Conserv. Genet.* 11 (5), 1737–1745. doi: 10.1007/s10592-010-0067-y
- Li, H., and Durbin, R. (2011). Inference of human population history from individual whole-genome sequences. *Nature* 475, 493–496. doi: 10.1038/nature10231
- Li, Y., Song, N., Khan, F. S., Yanagimoto, T., and Gao, T. (2013). New evidence of morphological characters and DNA barcoding of *Pampus argenteus* (Euphrasen 1788). *J. Fish. China* 37, 11. doi: 10.3724/SP.J.1231.2013.38824
- Li, Y., Song, N., Lin, L., and Gao, T. (2016). The complete mitochondrial genome of *Pampus echinogaster* (Perciformes: Stromateidae). *Mitochondrial. DNA. A. DNA. Mapp. Seq. Anal.* 27 (1), 289–290. doi: 10.3109/19401736.2014.892081
- Li, J., Xue, L., Cao, M., Zhang, Y., Wang, Y., Xu, S., et al. (2020). Gill transcriptomes reveal expression changes of genes related with immune and ion transport under salinity stress in silvery pomfret (*Pampus argenteus*). *Fish. Physiol. Biochem.* 46 (4), 1255–1277. doi: 10.1007/s10695-020-00786-9
- Liu, J., and Li, C. S. (2013a). A new species of the genus *Pampus* (Perciformes, Stromateidae) from China. *Acta Zootaxonomica Sinica* 38 (4), 885–890.
- Liu, J., and Li, C. S. (2013b). Identity of silver pomfret *Pampus argenteus* (Euphrasen1788) based on specimens from its type locality with a neotype designation (Teleostei Stromateidae). *Acta Zootaxonomica Sinica* 38 (1), 171–177.

- Liu, C., Li, Y., Chen, S., Song, N., and Gao, T. (2015). The complete mitochondrial genome of *Pampus punctatissimus* (Perciformes: Stromateidae). *Mitochondr. DNA* 26 (4), 649–650. doi: 10.3109/19401736.2013.836518
- Liu, B., Shi, Y., Yuan, J., Hu, X., Zhang, H., Li, N., et al. (2013). Estimation of genomic characteristics by analyzing k-mer frequency in *de novo* genome projects. *Quant. Biol.* 35 (s 1–3), 62–67. doi: 10.48550/arXiv.1308.2012
- Lu, M., An, H., and Li, L. (2016). Genome survey sequencing for the characterization of the genetic background of *Rosa roxburghii* trutt and leaf ascorbate metabolism genes. *PLoS One* 11 (2), e0147530. doi: 10.1371/journal.pone.0147530
- Luo, R., Liu, B., Xie, Y., Li, Z., Huang, W., Yuan, J., et al. (2012). SOAPdenovo2: an empirically improved memory-efficient short-read *de novo* assembler. *GigaScience* 1 (1), 18. doi: 10.1186/2047-217X-1-18
- Marçais, G., and Kingsford, C. (2011). A fast lock-free approach for efficient parallel counting of occurrences of k-mers. *Bioinformatics* 27 (6), 764–770. doi: 10.1093/bioinformatics/btr011
- Prost, S., Petersen, M., Grethlein, M., Hahn, S. J., Kuschik-Maczollek, N., Olesiuk, M. E., et al. (2020). Improving the chromosome-level genome assembly of the siamese fighting fish (*Betta splendens*) in a university master's course. *G3 Genes Genom. Genet.* 10 (7), 2179–2183. doi: 10.1534/g3.120.401205
- Ranallo-Benavidez, T. R., Jaron, K. S., and Schatz, M. C. (2020). GenomeScope 20 and Smudgeplot for reference-free profiling of polyploid genomes. *Nat. Commun.* 11, 1432. doi: 10.1038/s41467-020-14998-3
- Shao, F., Han, M., and Peng, Z. (2019). Evolution and diversity of transposable elements in fish genomes. *Sci. Rep.* 9 (1), 15399. doi: 10.1038/s41598-019-51888-1
- Simão, F. A., Waterhouse, R. M., Ioannidis, P., Kriventseva, E. V., and Zdobnov, E. M. (2015). BUSCO: assessing genome assembly and annotation completeness with single-copy orthologs. *Bioinformatics* 31 (19), 3210–3212. doi: 10.1093/bioinformatics/btv351
- Simpson, J. T. (2014). Exploring genome characteristics and sequence quality without a reference. *Bioinformatics* 30 (9), 1228–1235. doi: 10.1093/bioinformatics/btu023
- Song, H., Zhang, Y. X., Yang, M. J., Sun, J. C., Zhang, T., and Wang, H. Y. (2018). Genome survey on invasive veined rapa whelk (*Rapana venosa*) and development of microsatellite loci on large scale. *J. Genet.* 97 (4), e79–e86. doi: 10.1007/s12041-018-0975-z
- Van Dam, M. H., Henderson, J. B., Esposito, L., and Trautwein, M. (2021). Genomic characterization and curation of UCEs improves species tree reconstruction. *Syst. Biol.* 70 (2), 307–321. doi: 10.1093/sysbio/syaa063
- Wang, Q., Zeng, J., Wang, Y., Zhao, J., Ma, L., Shi, Z., et al. (2021). Alternations in the liver metabolome skin and serum antioxidant function of silver pomfret (*Pampus Argenteus*) is induced by jellyfish feeding. 3. *Biotech.* 11 (4), 192. doi: 10.1007/s13205-021-02702-1
- Wei, J., Wu, R., Xiao, Y., Zhang, H., Jawad, L. A., Wang, Y., et al. (2021). Validity of *Pampus liuorum* Liu & Li 2013, revealed by the DNA barcoding of *Pampus* fishes (Perciformes Stromateidae). *Diversity* 13, 618. doi: 10.3390/d13120618
- Will, C. L., and Lührmann, R. (2011). Spliceosome structure and function. *CSH. Perspect. Biol.* 3 (7), a003707. doi: 10.1101/cshperspect.a003707
- Xu, S., Zhang, H., and Gao, T. (2020). Comprehensive whole genome survey analyses of male and female brown-spotted flathead fish *Platycephalus* sp1. *Genomics* 112 (6), 4742–4748. doi: 10.1016/j.ygeno.2020.08.030
- Yang, Y., Li, Y., Wang, Y., Hu, J., Zhang, M., Sun, Y., et al. (2021a). The ultrastructure of spermatogenic cells and morphological evaluation of testicular development in the silver pomfret (*Pampus argenteus*). *Anat. Histol. Embryol.* 50 (6), 1034–1042. doi: 10.1111/ahc.12747
- Yang, Y., Ning, C., Li, Y., Wang, Y., Hu, J., Liu, Y., et al. (2021b). Dynamic changes in mitochondrial DNA morphology and fission during oogenesis of a seasonal-breeding teleost *Pampus argenteus*. *Tissue. Cell* 72, 101558. doi: 10.1016/j.tice.2021.101558
- Yin, G., Pan, Y., Sarker, A., Baki, M. A., Kim, J. K., Wu, H., et al. (2019). Molecular systematics of *Pampus* (Perciformes: Stromateidae) based on thousands of nuclear loci using target-gene enrichment. *Mol. Phylogenet. Evol.* 140, 106595. doi: 10.1016/j.ympev.2019.106595
- Zhang, M., Hu, J., Zhu, J., Wang, Y., Zhang, Y., Li, Y., et al. (2022). Transcriptome antioxidant enzymes and histological analysis reveal molecular mechanisms responsive to long-term cold stress in silver pomfret (*Pampus argenteus*). *Fish. Shellfish. Immunol.* 121, 351–361. doi: 10.1016/j.fsi.2022.01.017
- Zhao, X., Liu, Y., Du, X., Ma, S., Song, N., and Zhao, L. (2022). Whole-genome survey analyses provide a new perspective for the evolutionary biology of shimofuri goby *Tridentiger bifasciatus*. *Animals* 12 (15), 1914. doi: 10.3390/ani12151914
- Ziya Motalebipour, E., Kafkas, S., Khodaeiaminjan, M., Çoban, N., and Gözel, H. (2016). Genome survey of pistachio (*Pistacia vera* L.) by next generation sequencing: development of novel SSR markers and genetic diversity in *Pistacia* species. *BMC Genomics* 17 (1), 998. doi: 10.1186/s12864-016-3359-x